Chapter number

Hydrides of Cu and Mg Intermetallic Systems: Characterization and Catalytic Function

Maria H. Braga, Michael J. Wolverton, Maria H. de Sá and Jorge A. Ferreira
[1]*LANSCE, Los Alamos National Laboratory,*
[2]*CEMUC, Engineering Physics Department, FEUP, Porto University,*
[3]*LNEG,*
[1]*USA*
[2, 3]*Portugal*

1. Introduction

The worldwide demand for energy in the 21st century is growing at an alarming rate. The European "World Energy Technology and Climate Policy Outlook" [WETO] predicts an average growth rate of 1.8% per annum for the period 2000-2030 for the world energy demand (European Commission, 2003). The increased demand is being met largely by reserves of fossil fuel that emit both greenhouse gases and other pollutants. Since the rate of fossil fuel consumption is higher than the rate of fossil fuel production by nature, these reserves are diminishing and they will become increasingly expensive.

Against this background, the transition towards a sustainable, carbon-free and reliable energy system capable of meeting the increasing energy demands becomes imperative. Renewable energy resources, such as wind, solar, water, wave or geothermal, can offer clean alternatives to fossil fuels. Despite of their obvious advantages renewable energy sources have also some drawbacks in their use because they are unevenly distributed both over time and geographically. Most countries will need to integrate several different energy sources and an advanced energy storage system needs to be developed.

1.1 Hydrogen storage: A brief overview

Hydrogen has also attracted intensive attention as the most promising secure energy carrier of the future (Jain, 2009) due to its prominent advantages such as being:

1. Environmentally friendly. It is a "clean, green" fuel because when it burns in oxygen there is no pollutants release, only heat and water are generated:

$$2H_2\,(g) + O_2\,(g) \leftrightarrows 2H_2O\,(g)\,,\ \triangle H = 120\ kJ/g\ H_2 \qquad (1)$$

2. Easy to produce. Hydrogen is the most abundant element in the Universe and is found in great abundance in the world, allowing it to be produced locally and easily from a great variety of sources like water, biomass and organic matter;
3. Light. Hydrogen is the Nature's simplest and lightest element with only one proton and one electron with high energy per unit mass.

Nonetheless, opposing to the advantages of hydrogen as an energy carrier is the difficulty in storing it. Hydrogen storage remains a problem, in particular for mobile/vehicular applications (Felderhoff et al., 2007). High-pressure hydrogen gas requires very large volumes compared to petrol, for producing the same amount of energy. On the other hand, liquid hydrogen storage systems are not viable for vehicular applications due to safety concerns in addition to volumetric constraints. Thus, hydrogen storage viability has prompted an extensive effort to develop solid hydrogen storage systems but no fully satisfactory solutions have been achieved to date (Churchard et al., 2011).

The goal is to find a material capable of simultaneously absorbing hydrogen strongly enough to form a stable thermodynamic state, but weakly enough to release it on-demand with a small temperature rise (Jeon et al., 2011) in a safe, compact, robust, and efficient manner. There have been many materials under development for solid hydrogen storage, including metal hydrides (MH_x), via the chemical reaction of H_2 with a metal or metal alloy (M):

$$(x/2)\ H_2\ (g) + M\ (s) \leftrightarrows MH_x\ (s) \quad (2)$$

Generally, a typical hydriding reaction is known to involve several steps: (1) gas permeation through the particle bed, (2) surface adsorption and hydrogen dissociation, (3) migration of hydrogen atoms from the surface into the bulk, (4) diffusion through the particle and finally (5) nucleation and growth of the hydride phase. Any delay in one of these steps will reduce the kinetic properties of the process (Schimmel et al., 2005).

1.2 Magnesium hydride

Magnesium-based hydrogen storage alloys have been considered most promising solid hydrogen storage materials due to their high gravimetric hydrogen storage densities and volumetric capacity (see Table 1 adapted from (Chen & Zhu, 2008) for comparison) associated to the fact that magnesium is abundant in the earth's crust, non toxic and cheap (Grochala & Edwards, 2004; Jain et al., 2010; Schlapbach & Züttel, 2001).

Metal	Hydrides	Structure	Mass %	P_{eq}, T
$LaNi_5$	$LaNi_5H_6$	Hexagonal	1.4	2 bar, 298 K
$CaNi_3$	$CaNi_3H_{4.4}$	Hexagonal	1.8	0.5 bar, 298 K
ZrV_2	$ZrV_2H_{5.5}$	Hexagonal	3.0	10^{-8} bar, 323 K
TiFe	$TiFeH_{1.8}$	Cubic	1.9	5 bar, 303 K
Mg_2Ni	Mg_2NiH_4	Monoclinic (LT) / Cubic (HT)	3.6	1 bar, 555 K
Ti-V-based	Ti-V-based-H_4	Cubic	2.6	1 bar, 298 K
Mg	MgH_2	Tetragonal	7.6	1 bar, 573 K

Table 1. Structure and hydrogen storage properties of typical metal hydrides

Magnesium can be transformed in a single step to MgH_2 hydride with up to 7.6 wt% of hydrogen with a volumetric storage efficiency of 110g H_2/l (Milanese et al., 2010a), according to:

$$Mg\ (s) + H_2\ (g) \leftrightarrows MgH_2\ (s) \quad (3)$$

Magnesium metal is hexagonal with $P6_3/mmc$ space group (α-structure) but the absorption of hydrogen induces a structural change into the tetragonal rutile-type structure α-MgH_2 ($P4_2/mnm$) (Aguey-Zinsou & Ares-Fernández, 2010) (see Fig. 1).

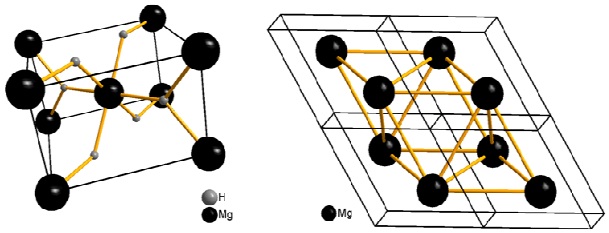

Fig. 1. Crystal structure of magnesium (left) and magnesium hydride (right) obtained with Materials Design® software

At high temperature and pressure, the latter phase undergoes polymorphic transformations to form two modifications: γ-MgH_2 and β-MgH_2, having an orthorhombic structure and a hexagonal structure, respectively (Schlapbach & Züttel, 2001). Other high-pressure metastable phases have also been reported (Cui et al., 2008; Ravindran et al., 2004). The charge density distribution in these materials has also been investigated and revealed a strong ionic character. The charge density determination of MgH_2 by means of synchrotron X-ray powder diffraction at room temperature, the maximum entropy method (MEM) and Rietveld refinement revealed that the ionic charge of Mg and H can be expressed by $Mg^{1.91+}$ and $H^{0.26-}$, respectively, denoting that Mg in MgH_2 is fully ionized, but the H atoms are in a weak ionic state (Noritake et al., 2003). The high strength of these bonds results however in an unacceptably high thermodynamic stability which diminishes the potentialities of using MgH_2 in practical applications. The hydrogen desorption temperature is well above 573 K, which is related to its high dissociation enthalpy (75 kJ/mol H_2) under standard conditions of pressure (Schlapbach & Züttel, 2001). In addition, the high directionality of the ionic bonds in this system leads to large activation barriers for atomic motion, resulting in slow hydrogen sorption kinetics (Vajo & Olson, 2007).

Several solutions were envisaged to circumvent these drawbacks. They can be accomplished to some extent by changing the microstructure of the hydride by ball-milling it (Huot et al., 1999; Zaluski et al., 1997). In this process the material is heavily deformed, and crystal defects such as dislocations, stacking faults, vacancies are introduced combined with an increased number of grain boundaries, which enhance the diffusivity of hydrogen into and out of the material (Suryanarayana, 2008). Alloying the system with other metallic additives, like 3d elements (Ti, Fe, Ni, Cu or Al), or $LaNi_5$, FeTi, Pd, V among others and oxides like V_2O_5 or Nb_2O_5 can also be a way of improving kinetic and/or thermodynamic properties by changing the chemical interaction between the atoms (Reule et al., 2000; Rude et al., 2011; Tan et al., 2011a). The use of a proper destabilization or catalyst element/alloy into the system has also been shown to improve adsorption/desorption kinetics and to lower the adsorption temperature (Beattie et al., 2011). Furthermore, substantial improvements in the hydriding-dehydriding properties can be achieved by nanoengineering approaches using nanosized reactants or by nanoconfinement of it (Jeon et al., 2011; Jurczyk et al., 2011; Vajo, 2011; Zaluska

et al., 1999a; Zhao-Karger et al., 2010). The latter allows shorter diffusion distances and larger surface area, resulting in faster reaction kinetics. It can also introduce alternative mechanisms to hydrogen exchange modifying the thermodynamic stability of the process.

As previously referred, an alternative approach for altering the thermodynamics of hydrogenation-dehydrogenation is achieved by using additives that promote hydride destabilization by alloy or compound formation in the dehydrogenated state. This approach is known as chemical destabilization. The principle underlying this approach is that the additives are capable to form compounds or alloys in the dehydrogenated state that are energetically favourable with respect to the products of the reaction without additives. Destabilization occurs because the system can cycle between the hydride and the additive instead of the elemental metal. A generalized enthalpy diagram illustrating this approach - destabilization of the generic hydride AH_2 through alloy formation (AB_x) promoted by the presence of the alloying species B - was given by Vajo and Olson (Vajo & Olson, 2007), and is shown in Fig. 2.

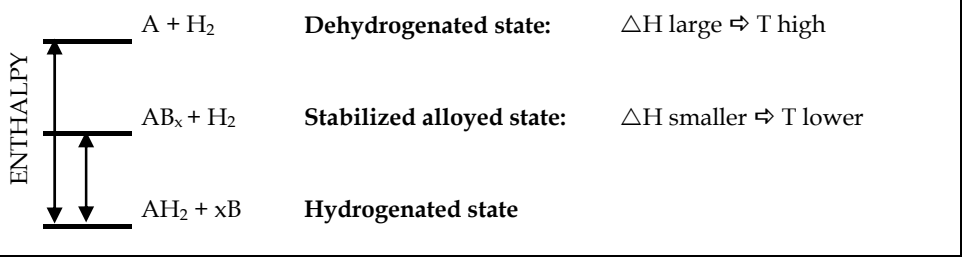

Fig. 2. Generalized enthalpy diagram illustrating destabilization through alloy formation upon dehydrogenation (adapted from Vajo & Olson, 2007)

1.3 Cu-Mg, Ni-Mg and other MgH_2 destabilizing systems

The work of Reilly and Wiswall provided the first evidences of this concept (Reilly & Wiswall, 1967, 1968). In their work, they showed that MgH_2 can be destabilized by Cu_2Mg. The formation of $CuMg_2$ occurs upon dehydrogenation at lower reaction temperatures than those obtained with just pure MgH_2. The compound $CuMg_2$ crystallizes in the orthorhombic structure (Braga et al., 2010c) and has a hydrogen capacity of 2.6 wt. % at 573 K (Jurczyk et al., 2007). The hydride formation enthalpy is approximately 5 kJ/mol H_2 lower than that of the hydrogenation of MgH_2 from Mg and this process obeys to the following scheme (Reilly & Wiswall, 1967):

$$2CuMg_2\,(s) + 3H_2\,(g) \leftrightarrows 3MgH_2\,(s) + Cu_2Mg\,(s) \quad (4)$$

The intermetallic cubic compound Cu_2Mg does not hydrogenate under conventional hydrogenation conditions and seems to improve dehydrogenation kinetics (as compared to MgH_2) due to improve resistance towards oxygen contamination (Andreasen et al., 2006; Kalinichenka et al., 2011; Reilly & Wiswall, 1967). As to the hexagonal intermetallic compound $NiMg_2$, Reilly and Wiswall (Reilly & Wiswall, 1968) established that it reversibly reacts with hydrogen to form a ternary hydride Mg_2NiH_4, with a hydrogen content of 3.6 wt. %, according to the following scheme:

$$NiMg_2\,(s) + 2H_2\,(g) \leftrightarrows NiMg_2H_4\,(s) \quad (5)$$

Results obtained by A. Zaluska and co-workers (Zaluska et al., 1999b) showed that ball-milling the mixtures MgH_2 and $NiMg_2H_4$ results in a synergetic effect of desorption, allowing the mixture to operate at temperatures as low as 493 K – 513 K, with good absorption / desorption kinetics and with total hydrogen capacity exceeding 5 wt.%. They point out however that the ball-milled mixtures of the hydrides behave differently from two metal phases that are firstly ball-milled and then hydrogenated. In the latter case volume changes occur during hydrogenation with associated volume expansion of the material, in contrast to what happen in their study in which $NiMg_2H_4$ promoted the hydrogen release from an adjacent MgH_2 matrix since they undergo a significant volume contraction, which facilitates their dehydrogenation.

Many more studies have focused on changes in the hydriding/dehydriding properties of Ni-Mg binary alloys with compositional changes and changes in processing variables. Nonetheless, we highlight the study of C. D. Yim and collaborators (Yim et al., 2007) that showed that the $NiMg_2$ compound acted as a catalyst in the dissociation of the hydrogen molecule, which resulted in a faster nucleation of magnesium hydride compared to pure Mg. It revealed also that the capacity and kinetics of hydriding were larger and faster when the average size of the hydriding phase was smaller and the volume fraction of the phase boundary was larger, since phase boundaries between the eutectic α-Mg and $NiMg_2$ phases acted as a fast diffusion path for atomic hydrogen.

In the full hydrogenated state, the $NiMg_2H_4$ structure consists of tetrahedral $[NiH_4]^{4-}$ complexes in a framework of magnesium ions and two different forms exist, high-temperature (HT) and low-temperature (LT). Under the partial pressure of 1 atm of hydrogen, the HT cubic structure phase transforms into a LT monoclinically distorted structure between 518 and 483 K (Zhang et al., 2009). The LT phase has also two modifications the untwined (LT1) and micro-twinned (LT2), which depend on the thermomechanical history of the sample (Cermak & David, 2011). The hydride formation enthalpy for the $NiMg_2H_4$ has been determined experimentally for the HT form, and it is in the range from -64.3 to -69.3 kJ/mol H2, for the LT form this value ranges from -68.6 to -81.0 kJ/mol H_2 (Tan et al., 2011b).

In the pioneer work of Reilly and Wiswall (Reilly & Wiswall, 1968) it was pointed out the catalytical effect of $NiMg_2$ on the hydrogen desorption characteristics of MgH_2. Recently, Cermak and David (Cermak & David, 2011) showed that $NiMg_2$, and more efficiently the LT1 phase of $NiMg_2H_4$, were responsible for the catalytic effect of Ni reported in the literature. The fact that $NiMg_2$ is a metal whereas $NiMg_2H_4$ behaves like a semiconductor has opened the way to the possibility of using this system also as a switchable mirror upon hydrogenation and dehydrogenation (Setten et al., 2007). A switchable mirror will switch from mirror to transparent material upon hydrogenation. A more detailed study of Ni-Mg-based hydrides can be found in (Orimo & Fujii, 2001).

Despite all the interest and extensive research on the above referred systems, a problem still remains; the hydrogen holding capacities of these materials are considerably less than that of MgH_2 (Sabitu et al., 2010). A way to overcome this limitation was found by combining MgH_2 with $LiBH_4$ (which involves the formation of MgB_2 and Li-Mg alloy (Yu et al., 2006)) since pure $LiBH_4$ has high gravimetric and volumetric hydrogen densities, 18.5 wt. % and

121 kg H_2/m^3, respectively (Bösenberg et al., 2010; Xia et al., 2011). However, although the reaction enthalpy is lowered and the hydrogen storage capacity increases (10.5 wt. %), the sorption and absorption processes occurs at high temperatures with relatively slow kinetic even though more additives are being tested in order to overcome this problem (Fernández et al., 2011; Xia et al., 2011). Alternatively, the study of the destabilization of MgH_2 with TiH_2 has also been taken experimentally (Choi et al., 2008; Sohn et al., 2011). Observations point to a substantially reduced apparent activation energy of 107-118 kJ/mol and significantly faster kinetics, compared with the 226 kJ/mol for the similarly milled MgH_2. The latter system constitutes a promising material to be used in practical applications for hydrogen storage.

The combined destabilization effect of Ni-Mg and Cu-Mg intermetallics towards MgH_2 was also tested and the Mg-rich ternary Cu-Ni-Mg alloys were recognized to have high potential for solid state hydrogen storage and have attracted many research interests. The study recently reported by Tan and co-workers (Tan et al., 2011b) elucidates about the influence of Cu substitution on the hydrogen sorption properties of magnesium rich Ni-Mg films. This study shows a two-step hydrogen absorption process. The first step is due to the absorption of Mg not alloyed in the form of $NiMg_2$ and/or $CuMg_2$, hereafter denoted as "free Mg" and is very quick, because it is mainly catalyzed by the intermetallic phase, $NiMg_2$. But the second step, due to the hydrogen absorption of intermetallic $NiMg_2$ and/or $CuMg_2$ ("bonded Mg") is significantly slow. The Cu substitution shows positive effects on desorption kinetics during full capacity hydrogen cycling, but shows strongly negative effects on absorption kinetics, particularly for the second absorption step, due to the segregation of $CuMg_2$ towards the grain boundaries of MgH_2, forming a closed shell that traps the hydrogen in MgH_2. The authors also reported that the Cu substitution has no thermo-destabilization for MgH_2, but since a significant amount can be dissolve in $NiMg_2$, even at elevated temperatures, thermo-destabilization of $NiMg_2H_4$ and better desorption kinetics are observed. Hong and collaborators (Hong et al., 2011) on their study on the hydrogen storage properties of x wt.% Cu-23.5 wt.% Ni-Mg (x = 2.5, 5 and 7.5) prepared by rapid solidification process and crystallization heat treatment have also reported that the $NiMg_2$ phase has higher hydriding and dehydriding rates than Mg under similar conditions and that the addition of a smaller amount of Cu is considered favourable to the enhancement of the hydriding and dehydriding rates of the sample. The 2.5 wt.% Cu-23.5 wt.% Ni-Mg alloy had the highest hydriding and dehydriding rates. These observations are in line with the ones previously reported by the group of Milanese (Milanese et al., 2010b; 2008), who also observed the high sorption capacity and good sorption performance of Cu-Ni-Mg mixtures and proposed a two steps sorption process with different kinetics. The first step corresponds to the quick hydrogenation of "free Mg", according to reaction (3). After this step, absorption keeps on with a slower rate corresponding to the second step, hydrogenation of the "bonded Mg" phases, $NiMg_2$ and $CuMg_2$, according to reactions (4) and (5). They also showed that Ni is more effective than Cu in catalyzing the desorption reactions and that $NiMg_2H_4$ and Cu_2Mg phases destabilized each other with the beneficial effect of decreasing the dissociation temperature of about 50 K in comparison to the MgH_2, from "free Mg". The positive effect of Cu as a catalyst on the hydrogenation and thermodynamic properties of $NiMg_2$ mixed by ball milling technique was also studied and recently reported by Vyas and co-workers (Vyas et al., 2011) showing that hydrogen storage capacity and enthalpy of formation of $NiMg_2$ with 10 wt.% Cu reduces to 1.81 wt.% and 26.69 kJ $(mol\ H)^{-1}$ from 3.56 wt.% and 54.24 kJ $(mol\ H)^{-1}$ for pure $NiMg_2$ at 573 K,

respectively. They attributed the decrement in the absorption capacity to the formation of the intermetallic phase Cu_2Mg, which does not absorb the hydrogen but itself behaves like a catalyst. However, in the case of nanocrystalline $Cu_xNi_{10-x}Mg_{20}$ (x = 0 - 4) alloys synthesized by melt-spinning technique, it was found (Zhang et al., 2010a, 2010b) that the substitution of Ni by Cu does not change the major phase $NiMg_2$ although it leads to a refinement of grains with increased cell volume and the formation of a secondary phase $CuMg_2$. This in turn leads to a decrease of the hydride stability with a clear improve of the hydrogen desorption capacity and kinetics of the alloys. The presence of $CuMg_2$ seems to act as a catalyst for the hydride-dehydride reactions of Mg and Mg-based alloys. Similar behaviour was found in $Cu_{0.25}Ni_{0.75}Mg_2$ and $Cu_{0.4}Ni_{0.6}Mg_2$ alloys that were prepared by mechanical alloying and subsequent thermal treatment (Simičić et al., 2006). The latter effect was also investigated on $Cu_{1-x}Ni_xMg_2$ (x = 0 - 1) alloys by Hsu and collaborators (Hsu et al., 2010). They observed that by substituting Cu by Ni in $CuMg_2$, the cell volume decreased (since the radius of Cu atom is slightly larger than Ni atom) and with increasing Ni content , the effect of Ni is actually effective in MgH_2 and Mg_2NiH_4 destabilization, leading to a decrease of desorption temperature in these two phases. They also showed that substituted nickel caused the hydriding reaction because absorption kinetics and hydrogen storage capacity increased with the rise of Ni-substitution contents.

1.4 Lithium hydride

An alternative route to be considered is to explore other hydrates besides MgH_2 for solid hydrogen storage. One of most interesting is lithium hydride, because it contains 12.5 wt.% hydrogen. Nonetheless, the desorption temperature is 1183 K for an equilibrium pressure of 1 bar (Vajo et al., 2004). However, it has been shown (Chen et al., 2003) that when LiH (see Fig. 3) reacts with lithium amide ($LiNH_2$) by thoroughly mixing the substances, hydrogen is released at temperatures around 423 K, with formation of lithium imide (Li_2NH) or Li-rich imide (Li_xNH_{3-X}) and lithium nitride (Li_3N) depending on the temperature and molar ratio of ($LiH/LiNH_2$) according to the following schemes:

- Below 593 K: $$LiH\ (s) + LiNH_2\ (s) \rightarrow 2H_2\ (g) + Li_2NH\ (s) \quad (6)$$

$$2LiH\ (s) + LiNH_2\ (s) \rightarrow (x\text{-}1)\ H_2\ (g) + Li_xNH_{3-X}\ (s) + (3\text{-}x)\ LiH(s) \quad (7)$$

- At higher temperatures: $$2LiH\ (s) + LiNH_2\ (s) \rightarrow H_2\ (g) + Li_3N\ (s) \quad (8)$$

From a detailed analysis of high-resolution synchrotron x-ray diffraction data for the lithium amide ($LiNH_2$) - lithium imide (Li_2NH) hydrogen storage system (David et al., 2007), the authors were able to propose an alternative mechanism that does not need to have the materials mechanically milled to enhance mixing, as previously recognized by Chen and collaborators (Chen et al., 2003) as essential. The mechanism they propose for the transformation between lithium amide and lithium imide during hydrogen cycling is a bulk reversible reaction that occurs in a non-stoichiometric manner within the cubic anti-fluorite-like Li-N-H structure, based on both Li^+ and H^+ mobility within the cubic lithium imide. Concluding that increasing the Li+ mobility and/or disorder it is likely to improve the hydrogen cycling in this and related Li-based systems. Recently, further systematical evaluation of the decompositions of $LiNH_2$ and Li_2NH was carried out by Zhang and Hu (Zhang & Hu, 2011), who also examined the effect of Cl^- anion on the decomposition

process. Cl^- is widely employed as a promoter to improve various catalysts. As a result, decomposition mechanisms were established. The decomposition of $LiNH_2$ producing Li_2NH and NH_3 occurs in two steps at the temperature range of 573-723 K. $LiNH_2$ decomposes into a stable intermediate species ($Li_{1.5}NH_{1.5}$) and then into Li_2NH. Furthermore, Li_2NH is decomposed into Li, H_2, and N_2 without formation of Li_3N at the temperature range of 823-1023 K. The introduction of Cl^- can decrease the decomposition *temperature of Li_2NH by about 110 K.*

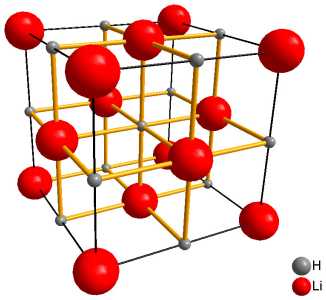

Fig. 3. Crystal structure of lithium hydride obtained with Materials Design® software

1.5 Neutron techniques associated with hydrogen solid storage

Though some progress have been made, the state-of-art materials are still far from meeting the aimed targets for hydrogen solid storage material (Churchard et al., 2011). This huge task can be facilitated by employing state-of-the-art techniques like, computational first-principles calculations to evaluate the thermodynamic properties of the potential materials (Alapati et al., 2007; Siegel et al., 2007; Yang et al., 2007). This allows a quick screen of a large number of potential candidates, searching for thermodynamically suitable ones (saving time and money). Once thermodynamic appropriate materials have been found other considerations such as structure and dynamics of the materials during hydrogenation/dehydrogenation will become crucial in order to understand the fundamental properties of hydrogen storage, in realistic conditions and hence design new hydrogen storage materials.

Neutron scattering techniques are highly suitable for structure and dynamics studies related to hydrogen in solids and bound on surfaces. The energy distribution of thermal neutrons is nearly ideal for the study of condensed matter in general because it is of the same order of magnitude as most molecular and lattice excitations and the de Broglie wavelengths of thermal neutrons match quite well with interatomic distances in most solids (Squires, 1978). Neutrons have some unique advantages over photons and electrons as scattering media which are of particular use for the analysis of hydrides. For these purposes the two most useful neutron scattering interactions are coherent elastic scattering for Neutron Diffraction (ND) and incoherent Inelastic Neutron Scattering (INS) to measure vibrational density of states. The distinction of coherent and incoherent scattering interactions is important to the unique advantages offered by ND and INS respectively. This is because the relative scattering intensity of a given interaction is dependent highly upon the nucleus involved, and as such is isotope dependant. Each isotope has a different scattering cross section for both coherent (σ_{coh})

and incoherent (σ_{inc}) interactions measured in barns (1 barn = 10^{-28} m^2). In general these scattering cross sections do not follow any specific trend regarding nucleus size.

INS has numerous advantages to other common techniques of obtaining vibrational spectra such as infrared (IR) and Raman spectroscopy. INS spectroscopy is hyper sensitive to the presence of hydrogen. The protium (^1H) nucleus has respective scattering cross sections of σ_{coh} = 1.8 and σ_{inc} = 80.2 barns respectively. This means neutron scattering in materials containing natural abundance hydrogen is largely inelastic. Additionally, the incoherent cross section of ^1H is one to two orders of magnitude higher than any other isotope (Ross, 2008). This means that in hydrides INS spectra are dominated by vibrational modes of hydrogen almost exclusively. This hyper sensitivity to hydrogen means that hydride phases are detectible even when present in relatively miniscule concentration. Another advantage of INS is the complete absence of selection rules for the excitation of vibrational modes. lattice modes (i.e. phonons) are excited with equal opportunity to molecular vibrations. Because both IR and Raman spectroscopy rely upon different types of charge symmetry interactions, many materials have vibrational modes that cannot be excited by Raman or IR. In particular lattice modes are far more easily observable in INS spectra than any other type of vibrational spectroscopy. INS is also more useful for comparison with *ab initio* calculated density of states because relative excitation amplitudes are simply dependent upon the magnitude of motion and σ_{inc} of the excited nucleus (Squires, 1978; Ross, 2008). Free software, such as a-Climax is available to generate a theoretical INS spectrum from the density of states output files from numerous common *ab initio* packages such as Gaussian, AbInit and Dmol (Ramirez, 2004).

For these reasons INS is extremely useful in identifying the presence of different hydride phases which may not be structurally apparent (for example, due to structural disorder). A good example is the INS study of Schimmel et al. on MgH_2 produced from Mg processed by high energy ball milling. Ball milling of Mg to reduce particle size, and introduce fractures, defects, and faults has a beneficial effect of increasing hydride formation rate, and reducing the temperature required for absorption. Comparison of the INS spectra of the MgH_2 produced from ball milled Mg with well-ordered MgH_2 revealed a partial composition of γ-MgH_2, which is metastable and normally exists only at high temperatures (Schimmel et al, 2005). Presence of γ-MgH_2 was indicative of internal stress from mechanical processing. However after hydrogen sorption cycling, γ-MgH_2 was no longer observable in the INS spectrum of the ball milled material, while the fast kinetics and lower sorption temperature remained. In this way INS was indispensable in revealing that the particle size reduction is more significant in the role of lowering temperature and increasing sorption kinetics than the creation of faults and internal stresses after the high energy ball milling of Mg (Schimmel, 2005; Ross, 2008).

Neutron diffraction also provides some unique advantages versus more conventional diffraction methods such as X-ray diffraction (XRD). Elastic neutron and X-ray scattering are similar in that both result in interference patterns according to Bragg scattering conditions (Squires, 1978). In XRD the intensity of a given Bragg reflection varies with the atomic number (Z) of the atom at the lattice site. This means that the exact position of hydrogen in a structure is practically impossible to determine with XRD. In ND the relative intensities of reflections are independent of Z, and instead depend on the coherent scattering cross section (σ_{coh}). This means that deuterium (^2H; σ_{coh} = 5.6, σ_{inc} = 2.0) is just as readily observable as

most metal atoms. This allows for the observation of hydride phase transitions which differ only by the hydrogen occupation sites, such as in interstitial hydrides. ND also allows metals with similar Z values such as Ni (Z=28, σ_{coh} = 13.4) and Cu (Z=29, σ_{coh} = 7.5) to be easily distinguished, unlike in XRD. A great deal of caution must be taken to ensure that ^2H is not displaced by ^1H during sample preparation and handling, as the large σ_{inc} of ^1H will create a substantial background signal. Another advantage of ND is that intensity does not diminish greatly with scattering angle as it does in XRD (Massa, 2004). Beyond these differences, crystal structure determination techniques are very similar for ND and XRD. Common approaches include a combination of a structure solution method and the Rietveld refinement method.

ND and INS carry some common advantages and disadvantages intrinsic with the use of neutrons as a scattering medium. Common advantages are associated with the highly penetrating quality of neutron radiation through most materials. This provides some possibilities for variable depth of measurements. If the neutron beam is directed at a relatively thin portion of the sample, a greater quantity of surface and shallow depth material is surveyed, whereas in relatively thick segments predominantly material deep within the sample is surveyed. The high penetration of neutrons also allows for relatively clear in-situ measurements in a wide range of sample environments such as high pressure gas cells, furnaces, cryogenic refrigerators, anvil cells and other environments requiring obtrusive equipment. This allows for detailed structure and dynamics studies of metastable hydride phases, and phase transitions which occur only in extreme conditions.

There are numerous inconveniences associated with neutrons as well. The most prevalent and obvious is the relative scarcity and cost of neutron sources, which typically take two forms: a research reactor or a spallation source (fed by a high energy proton accelerator). Another drawback is the time required to conduct a measurement, which can range from several hours to several days (per measurement). This is due to the short range of nuclear forces and relatively low probability of a scattering event, which is the same reason neutron radiation penetrates so effectively. Because of the long measurement time and high operational cost beam time is allocated very carefully at neutron sources, and flight paths are rarely left idle during neutron production. ND and INS require larger sample sizes, often multiple grams, to increase the scatting rate.

2. Hydrides of Cu and Mg intermetallic systems

We have studied the Cu-Li-Mg system as a hydrogen storage system and, at the same time, as a catalyst of the hydrogen storage process, namely for the Ti/TiH_2 system (Braga & Malheiros, 2007a, 2007b; Braga et al., 2010a, 2010b). The only ternary compound the Cu-Li-Mg system holds is $CuLi_xMg_{2-x}$ (x = 0.08) with hexagonal $P6_222$ structure (Braga et al., 2010c). Since the phase diagrams of Cu-Mg and Ni-Mg are similar (see Fig. 4), and Cu and Ni have similar electron affinities, it was thought in the sixties that $CuMg_2$ would store hydrogen, too.

However this is not the case (Reilly & Wiswall, 1967). $NiMg_2$ has a hexagonal structure ($P6_222$), but $CuMg_2$ has an orthorhombic structure (Fddd), and this structural difference is assumed to be the reason that $NiMg_2$ stores H_2 forming a hydride, but $CuMg_2$ does not. $CuMg_2$ decomposes into Cu_2Mg and MgH_2 (Reilly & Wiswall, 1967) upon hydrogen loading

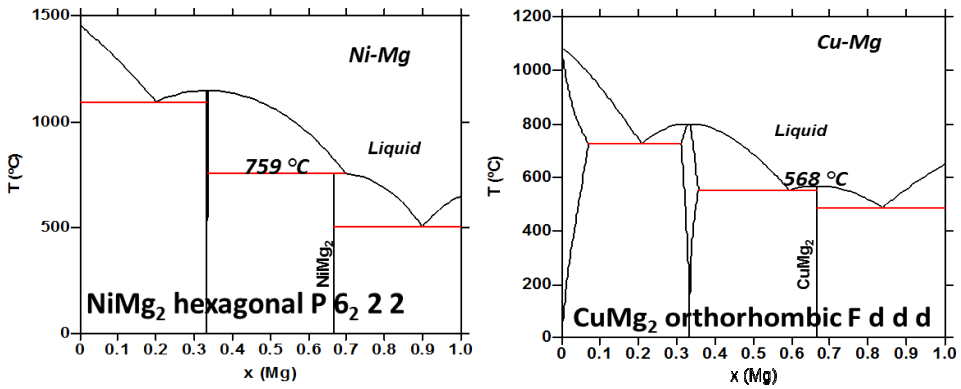

Fig. 4. Phase diagrams of Ni-Mg and Cu-Mg (Ansara et al., 1998)

as previously referred (4). As a result of this reaction and since $CuMg_2$ does not form a hydride, $CuMg_2$ was abandoned as a candidate material for hydrogen storage (Reilly & Wiswall, 1967; Schlapbach & Züttel, 2001) until the late destabilization studies that were previously cited. The hexagonal structure of $CuLi_xMg_{2-x}$, suggested the possibility of using this phase as a hydrogen storage material (Braga & Malheiros, 2007a, 2007b) because $CuLi_xMg_{2-x}$ has the same space group ($P6_222$) as $NiMg_2$ and $NiMg_2(H,D)_{0.3}$ (lattice parameters are almost identical: a = b = 5.250 Å and c = 13.621 Å (at 300 K) for $CuLi_xMg_{2-x}$ and a = b = 5.256 Å and c = 13.435 Å for $NiMg_2(H,D)_{0.3}$ (Senegas et al., 1984)). Therefore, we hypothesized that $CuLi_xMg_{2-x}$ (x = 0.08) would be a hydrogen storage material, just like $NiMg_2$ - a hypothesis that has been confirmed by now (Braga & Malheiros, 2007a, 2007b; Braga et al., 2010a).

The change of the $CuMg_2$ orthorhombic (Fddd) structure to a hexagonal structure ($P6_222$) upon addition of a small amount of Li has been firmly established (Braga et al., 2007). Isostructural phases to $CuLi_xMg_{2-x}$ are the hexagonal phase $NiMg_2$ and $NiMg_2H_{0.24-0.30}$ (Senegas et al., 1984). For the NiMg-hydrides, several hydrogen positions were reported: In $NiMg_2H_{0.29}$ the hydrogen atoms occupy Wyckoff 6f positions and could occupy the interstitial Wyckoff 6h position (Senegas et al., 1984). Other possibilities would be that the H atoms would just occupy interstitial Wyckoff 12k position (in $NiMg_2H_{0.26}$) or the Wyckoff 12k and 6j positions in $NiMg_2H_{0.24}$ (Senegas et al., 1984). This suggests a number of possible sites for Li in $CuLi_xMg_{2-x}$.

Interestingly V. Hlukhyy and collaborators (Hlukhyy et al., 2005) have reported a result closely related to our observations in the Sn-doped Ni-Mg system. These authors show that the synthesis of alloys in the Ni-Mg system is affected by the presence of small amounts of Sn (forming $NiMg_{2-x}Sn_x$ with x = 0.22 and 0.40). The replacement of Mg by Sn produces changes in the structure of $NiMg_2$, this time making the alloy change from the $NiMg_2$ type (hexagonal) to the $CuMg_2$ type (orthorhombic). While the structure of $NiMg_{1.85}Sn_{0.15}$ is still of $NiMg_2$ type, the structure of $NiMg_{1.78}Sn_{0.22}$ and $NiMg_{1.60}Sn_{0.40}$ is already of the $CuMg_2$ type. These results represent obviously the converse of our own observations in the $CuMg_2$ structure, and reaffirm our results with respect to $CuLi_xMg_{2-x}$.

2.1 The $CuLi_{0.08}Mg_{1.92}$ compound

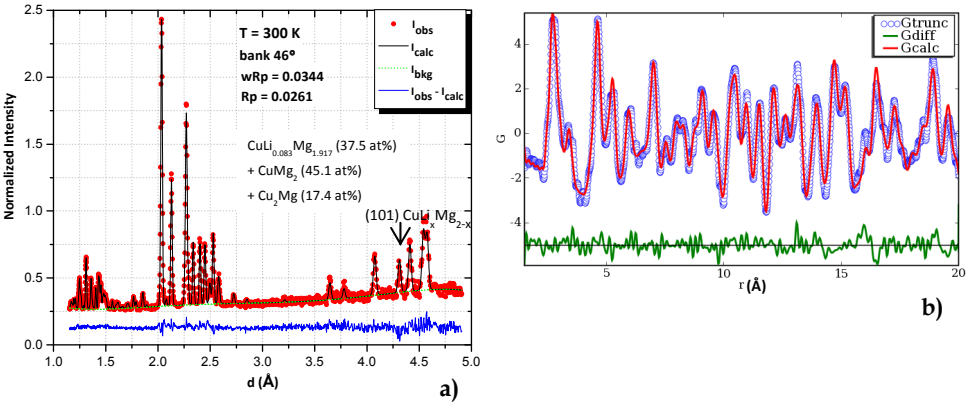

Fig. 5. a) Neutron diffraction pattern of a sample containing $CuLi_{0.08}Mg_{1.92}$, $CuMg_2$ and $CuMg_2$. The highlighted peak corresponds to the (101) reflection for the $CuLi_{0.08}Mg_{1.92}$ compound which is not overlapped by other phases. b) Pair Distribution Function (PDF) fitting for the same conditions of the pattern in a).

We have used neutron diffraction to refine the composition of $CuLi_xMg_{2-x}$, site occupancies and lattice parameters at different temperatures. In Fig. 5, results from the Time-of-flight (TOF) Neutron Powder Diffractometer (NPDF) at the Los Alamos Neutron Science Center (LANSCE) are shown. It was analyzed a sample containing 37.5 at.% of $CuLi_{0.08}Mg_{1.92}$, 45.1 at.% of $CuMg_2$ and 17.4 at.% of Cu_2Mg. The structure was refined using the General Structure Analysis System (GSAS), a Rietveld profile analysis program developed by A. C. Larson and R. B. von Dreele (Larson & von Dreele, 2004).

Furthermore, we've fitted the NPDF data using the Pair Distribution Function (PDF) in which G(r) was obtained via the Fourier Transform of the total diffraction pattern as indicated below:

$$G(r) = 4\pi r\left[\rho(r) - \rho_0\right] = \frac{2}{r}\int_0^{\infty} Q\left[S(Q) - 1\right]\sin(Qr)\,dQ \tag{9}$$

where $\rho(r)$ is the microscopic pair density, ρ_0 is the average atomic number density, and r the radial distance. Q is the momentum transfer ($Q = 4\pi\sin(\theta)/\lambda$). $S(Q)$ is the normalized structure function determined from the experimental diffraction intensity (Egami & Billinge, 2003). PDF yields the probability of finding pairs of atoms separated by a distance r. PDF fittings were performed using the software PDFgui (Farrow et al., 2007).

Besides Neutron Diffraction, we have used theoretical complementary methods to determine the stoichiometry of the $CuLi_xMg_{2-x}$ compound. We relied on the Density Functional Theory (DFT) (Hohenberg & Kohn, 1964) to calculate the structure that minimized the Electronic Energy at 0 K, without accounting for the zero point energy. The latter energy gives us a good estimation of the Enthalpy of Formation at 0 K especially since we were relating data for stoichiometries that did not differ too much and for similar crystal structures. The results

obtained are in close agreement with those obtained from ND after Rietveld refinement - $CuLi_xMg_{2-x}$ (x = 0.08). Nonetheless, no conclusions about Li site occupancies could be drawn from the use of the referred means. DFT shows that there isn't a clear preference, in terms of energy, for the different Li site occupancies. Then again, a technique that gives information about the average site occupancies - like the Rietveld refinement - is also inadequate to clarify this problem; therefore we have used PDF to determine Li preferred sites. With PDF fittings we were allowed to go further (see Fig. 5b). PDF does not see the average but the local structure and with PDF, all results but those in which Li would substitute Mg1 sites (1/2, 0, z), gave negative occupancies for Li. For Li substituting Mg1 we've obtained an average composition for $CuLi_xMg_{2-x}$ (x = 0.07) which is in agreement with the other obtained results. For further information please see (Braga et al., 2010c).

2.2 Hydrogen storage in the Cu-Li-Mg-H(D) system

To study the hydrogen storage in the Cu-Li-Mg system several techniques were used (Braga et al., 2010a). Besides absorption/desorption, Differential Scanning Calorimetry, Thermal Gravimetry Analysis (DSC/TGA), X-ray Diffraction (XRD) both at the laboratory and at the Synchrotron, we have used Neutron Diffraction and Inelastic Neutron Scattering. Owing to the low X-ray scattering power of hydrogen, neutron diffraction experiments on deuterides are necessary as previously highlighted in section 1.5.

Most atomic arrangements were determined on powders of different samples yet we have also used a bulk sample machined into a cylinder to obtain ND data in both the surface and the center of the sample during deuterium uptake.

The data were usually analyzed by the Rietveld method, yet in some cases in which the background was noisier we have used the biased method (Larson & von Dreele, 2004). For better convergence, the number of refined parameters in particular those of the atomic displacement amplitudes are reduced by constraints.

ND results obtained from the High-Intensity Powder Diffractometer HIPD at LANSCE, Los Alamos National Laboratory, for a sample initially containing 78 wt.% $CuLi_{0.08}Mg_{1.92}$ + 22 wt.%Cu_2Mg (from here on "initially containing" means before hydrogen/deuterium absorption) and that was deuterated *ex situ* at 473 K at P ≤ 50 atm in order to determine the crystal structure of the first deuteride phase formed in the sample (see Fig. 6 left). This pattern was refined using Rietveld's method.

The $CuLi_{0.08}Mg_{1.92}D_5$ crystal structure was determined to be monoclinic P121, with a = 15.14 Å, b = 6.88 Å, c = 5.55 Å and β = 91.73° according to the formula $CuLi_{0.08}Mg_{1.92}D_5$ = $0.5(Mg_3^{2+}.[CuH_4]_2^{3-}.MgD_2)$ corresponding to 4.4 wt% D per formula unit. $CuLi_{0.08}Mg_{1.92}D_5$ is the first deuteride/hydride to be formed. This result is interesting by itself, but the presence of MgD_2 in the diffraction pattern, highlights even further the possibilities of applications of this compound. According to these results, it can be obtained $MgH(D)_2$ from a sample that did not contain "free" Mg or $CuMg_2$. Furthermore, the deuteration process occurred at 473 K, which is considerably lower than the hydrogen absorption temperature reported for $CuMg_2$ (4) (Reilly & Wiswall, 1967).

The experiments with the bulk sample at SMARTS, LANSCE, Los Alamos National Laboratory, show that before MgD_2 is observed, $CuLi_{0.08}Mg_{1.92}D_5$ is already distinguishable at the surface even in a sample that initially contained $CuMg_2$ (see Fig. 7). Therefore, it

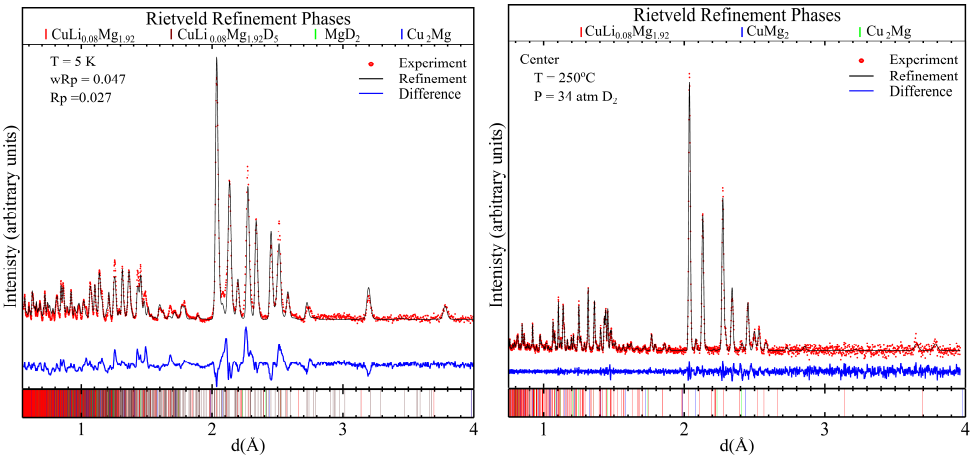

Fig. 6. (left) Rietveld refinement of a sample containing $CuLi_{0.08}Mg_{1.92}$, Cu_2Mg, MgD_2 and $CuLi_{0.08}Mg_{1.92}D_5$ obtained in HIPD. wRp and Rp are the reliability factors as defined in (Larson & von Dreele, 2004). (right) ND pattern of the center of a bulk cylinder sample containing $CuLi_{0.08}Mg_{1.92}$, Cu_2Mg, $CuMg_2$ obtained from the Spectrometer for Materials Research at Temperature and Stress SMARTS during an *in situ* reaction with D_2 at 523 K and ~34 atm. Both patterns show experimental, refined and difference between experimental and calculated intensities.

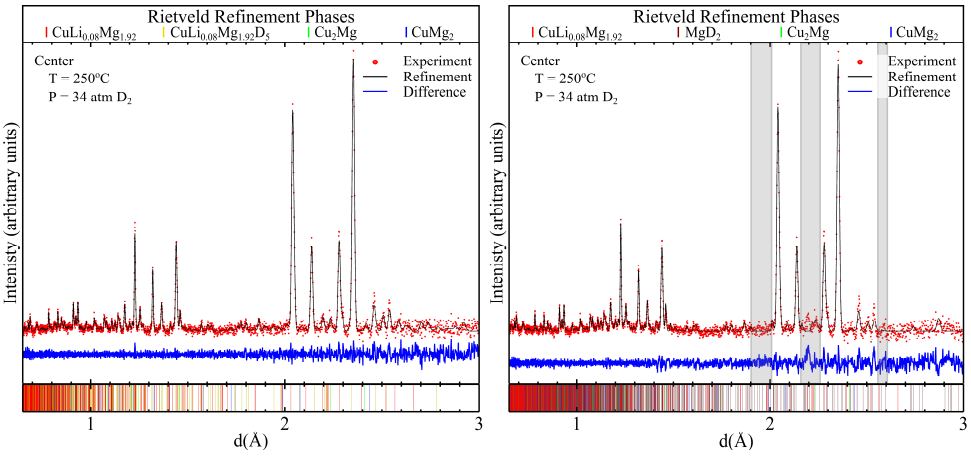

Fig. 7. (left and right) ND pattern of the surface of a bulk cylinder sample initially containing $CuLi_{0.08}Mg_{1.92}$, Cu_2Mg, and $CuMg_2$ obtained in SMARTS during an *in situ* reaction with D_2 at 523 K and ~34 atm. (right) it is highlighted that MgD_2 cannot justify some existing peaks. Both patterns show experimental, refined and difference between experimental and calculated intensities.

seems that $CuLi_{0.08}Mg_{1.92}D_5$ will have a catalytic and destabilizing roll that was additionally observed with the Ti/TiH_2 systems (Braga et al., 2010b).

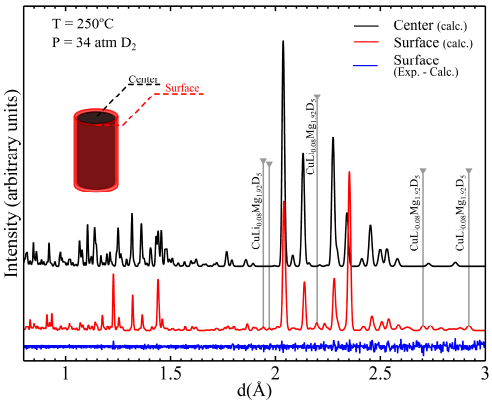

Fig. 8. ND refined pattern of the center and surface of a bulk cylinder sample initially containing $CuLi_{0.08}Mg_{1.92}$, Cu_2Mg, and $CuMg_2$ obtained in SMARTS during an *in situ* reaction with D_2 at 523 K and ~34 atm. Besides the texture effect that might be present in a bulk sample, it seems that the center initially contained more $CuLi_{0.08}Mg_{1.92}$ than the surface.

Experimental information about the metal–hydrogen interactions can be obtained by measuring lattice vibrations via INS, as previously highlighted in section 1.5. Because of the large difference between the masses of metal and H atoms in transition-metal–hydrogen systems, the acoustic dispersion branches of the phonon spectra can be attributed to the motion of the metal atoms, the optic branches to the vibrations of the light H atoms relative to the metal lattice. The densities of states of optic phonons typically show a pronounced maximum at the energy of the lattice vibrations at the Γ point in the centre of the phonon Brillouin zone (q = 0) e.g. in (Fukay, 1993). These phonon modes describe the vibration of the undistorted H sublattice relative to the rigid metal sublattice. Hence, they contain the metal–hydrogen interaction only. This is usually stronger than the H–H interaction, which leads to the dispersion of the optic branches. In the limit of very low H concentrations, the H vibrations can be imagined as independent vibrations of local Einstein oscillators at interstitial H sites. For both the lattice vibrations at the Γ point and the local vibrations, one can observe transitions from the ground state, the quantum-mechanical zero-point vibration of the H atoms, to the first excited states, e.g. by measuring optic phonon excitations, and transitions to higher excited states. Their energies, intensities and symmetry splittings yield an insight into the shapes of the potential and the wavefunctions for the vibrations of the light particles (Elsasser et al., 1998).

We have measured samples of the Cu-Li-Mg-H system by means of INS measured with the Filter Difference Spectrometer FDS, at LANSCE, Los Alamos National Laboratory. There is no doubt about the sequence of events; first there is the formation of $CuLi_{0.08}Mg_{1.92}H_5$ (see Fig. 9a) and then in subsequent cycles the formation of MgH_2 (see Fig. 9b), either for disproportionation of $CuLi_{0.08}Mg_{1.92}H_5$ or from hydrogenation of $CuMg_2$.

DSC/TGA experiments show that $CuLi_{0.08}Mg_{1.92}H_5$ starts desorbing hydrogen at 313 K to 328 K. In this range of temperatures the sample can release up to 1.3 wt.% (results for a isothermal experiment with a sample initially containing approximately 78 wt.% of $CuLi_{0.08}Mg_{1.92}$ and 22 wt.% of Cu_2Mg - which does not absorb hydrogen at the temperature and pressure that were used). In Fig. 10 it can be seen that 0.5 wt.% of a sample initially containing 61 wt.%

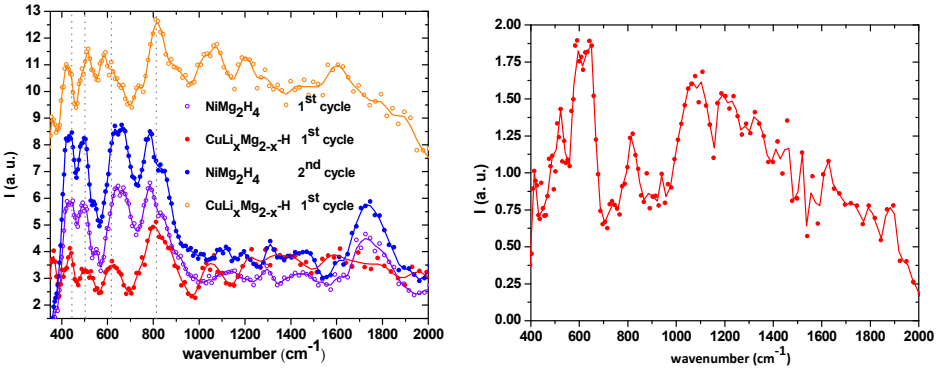

Fig. 9. a) INS spectra for $NiMg_2H_4$ (1st and 2nd hydrogenation cycles) and for two samples containing $CuLi_{0.08}Mg_{1.92}$ (close circles below correspond to a sample that also contained Cu_2Mg and the open circles above correspond to sample that contained Cu_2Mg and $CuMg_2$ as well). All samples show the formation of a similar monoclinic structure. As in $NiMg_2H_4$, in which Ni is bonded to four atoms of H forming the tetrahedral complex $[NiH_4]^{4-}$, Cu is also bonded to four atoms of H forming the tetrahedral complex $[CuH_4]^{3-}$, which was previously referred on (Yvon & Renaudin, 2005). b) Sample initially containing approximately 61 wt.% of $CuLi_{0.08}Mg_{1.92}$, 23 wt.% of $CuMg_2$ and 16 wt.% of Cu_2Mg, after the 3rd hydrogenation cycle at 473 K, and ~50 atm. It is clear the formation of MgH_2 with a peak at ~620 cm^{-1}.

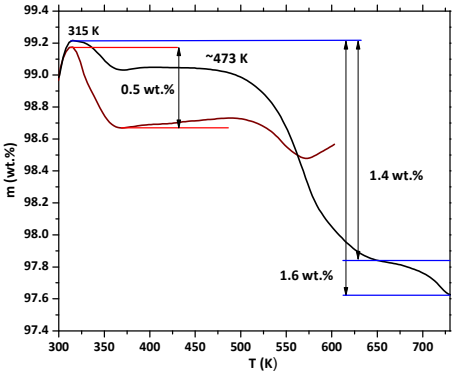

Fig. 10. TGA of two samples initially containing approximately 61 wt.% of $CuLi_{0.08}Mg_{1.92}$, 23 wt.% of $CuMg_2$ and 16 wt.% of Cu_2Mg. Samples were measured after hydrogenation but they are not expected to be saturated in hydrogen prior to the experiment.

of $CuLi_{0.08}Mg_{1.92}$, 23 wt.% of $CuMg_2$ and 16 wt.% of Cu_2Mg can be released at T < 350 K. In spite of the fact that there was some visible oxidation during this run, we think it was worth showing this initial desorption. This initial desorption seems to be due to $CuLi_{0.08}Mg_{1.92}H_5$. At ~473 K, hydrogen starts to be desorbed at a different rate, probably due to the disproportionation of $CuLi_{0.08}Mg_{1.92}H_5$, with the formation of MgH_2, which will start releasing hydrogen at 553-573 K. Additionally, MgH_2 can be formed upon hydrogenation of $CuMg_2$.

The DSC/TGA results show that the system containing $CuLi_{0.08}Mg_{1.92}$ and Cu_2Mg can destabilize MgH_2 in a more efficient way than Cu_2Mg by itself can. In fact, in a DSC experiment in which kinetics must be accounted for, MgH_2 will release hydrogen at 553-573 K, which can only be obtained when particles are reduced to nanopowders.

2.3 Hydrogen storage in the Cu-Li-Mg-H(D)+Ti system

A sample with 60.5 at% of $CuLi_{0.08}Mg_{1.92}$, 23.9 at% of $CuMg_2$ and 15.6 at% of Cu_2Mg was mechanically alloyed to titanium resulting into Cu-Li-Mg+Ti samples. The brittle CuLiMg alloy was mixed with Ti (99.9% purity, 325 mesh, Alfa Aesar) so that 68.2 at% / 47.3 wt% of the final mixture was Ti. The mixture was ball-milled for 3 h in a dry box under a He protective atmosphere. The Cu-Li-Mg+Ti mixture was then sealed inside a stainless steel crucible and kept at 473 K for 9h under D_2 at P = 34 bar. These samples were then cooled to 5 K (HIPD, neutron powder diffraction) over a period of 2 to 3 hours.

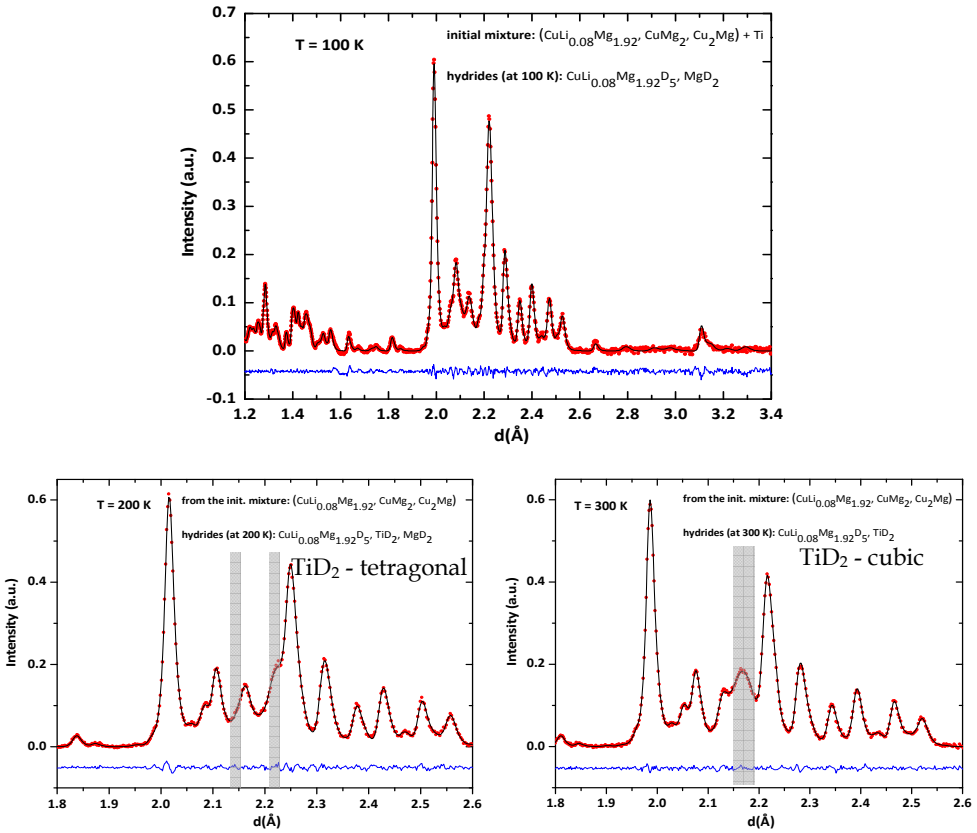

Fig. 11. Comparison of Cu-Li-Mg+Ti-D neutron diffraction pattern refinements from measurements taken at T= 100K, 200K, and 300K.

Cu-Li-Mg+Ti-D neutron diffraction samples were quenched and measured at the lowest temperature, 5K, first with 60K, 100K, 200K and 300K measurements taken subsequently. For diffraction patterns collected at 5K – 100K there is *no evidence* of any titanium deuteride phases. This is immediately obvious in Fig. 11 which shows a comparison of the 100, 200 and 300 K Cu-Li-Mg+Ti-D. Bragg peaks belonging to tetragonal TiD_2 begin to appear in the 200K pattern of the Cu-Li-Mg+Ti-D sample. The refinement at 100 K includes the 5 phases: $CuMg_2$, Cu_2Mg, $CuLi_{0.08}Mg_{1.92}$, $CuLi_{0.08}Mg_{1.92}D_5$ and α-Ti; at 200 K: $CuMg_2$, Cu_2Mg, $CuLi_{0.08}Mg_{1.92}$, $CuLi_{0.08}Mg_{1.92}D_5$ and MgD_2 plus tetragonal TiD_2 and at 300 K: $CuMg_2$, Cu_2Mg, $CuLi_{0.08}Mg_{1.92}$, $CuLi_{0.08}Mg_{1.92}D_5$ plus cubic TiD_2 and represents an excellent fit to the data as confirmed by the residual. At 300K a structural phase transition (tetragonal to cubic) occurs in TiD_2 (Yakel, 1958). The appearance of the TiD_2 cubic phase in the 300K diffraction pattern is confirmed by refinement as shown in Fig. 11.

Fig. 11 shows the changes in the Cu-Li-Mg+Ti-D sample as the temperature is increased from 100K to 300K: The $CuLi_{0.08}Mg_{1.92}D_5$, MgD_2 and α-Ti phases are progressively reduced in intensity while TiD_2 appears at 200K transforming from tetragonal to cubic at 300K. Since there was no further exposure of the sample to deuterium, the formation of TiD_2 must have been facilitated through *solid state diffusion* of deuterium from a separate phase. The decrease in intensity of Bragg peaks belonging to the Cu-Li-Mg-D phase implicates that the mechanism involves solid state transfer of deuterium from Cu-Li-Mg-D to Ti.

DSC/TGA measurements show the dehydrogenation of $CuLi_{0.08}Mg_{1.92}H_5$ accounts for approximately third of the total mass loss. Given that no other hydride phases were present in any significant quantity, and that MgH_2 began dehydrogenation at 553 K in the Cu-Li-Mg-H samples, the mass loss beginning at 590 K is due to the release of hydrogen from TiH_2. This demonstrates a significant catalytic effect for desorption as well given that TiH_2 ordinarily does not dissociate until well above 723 K (Gibb & Kruschwitz, 1950). For further information please check (Braga et al., 2010b).

3. Conclusion

The hydrogen storage world still offers a considerable amount of challenges since no universal solution has been found. Eventually, different solutions will be proposed to suite different applications.

The Cu-Li-Mg system provides other possibilities for catalytic and destabilization effects yet not fully explored.

There are several techniques that can be employed to study systems containing hydrogen. Nonetheless, Neutron Scattering is a very useful resource, in particular, Neutron Diffraction. In the latter, crystal structure of deuteride phases are directly studied since deuterium can be detected by ND and accurate results can be obtained either in *ex situ* or *in situ* experiments as shown previously.

4. Acknowledgments

The authors would like to acknowledge FCT – Portugal and FEDER - EU, for the PTDC/CTM/099461/2008 project. This work has benefited from the use of HIPD, NPDF, SMARTS and FDS at LANSCE, LANL, funded by DOE, DE-AC52-06NA25396. The authors

would like to acknowledge the Lujan Center's, LANSCE, instrument scientists for their support and helpful discussions.

5. References

Aguey-Zinsou, K. & Ares-Fernández, J. (2010). Hydrogen in magnesium: new perspectives toward functional stores. *Energy & Environmental Science,* Vol. 3, No. 5, (February 2010), pp. 526-543, ISSN 1754-5706

Alapati, S., Johnson, J. & Sholl, D. (2007). Using first principles calculations to identify new destabilized metal hydride reactions for reversible hydrogen storage. *Physical Chemistry Chemical Physics,* Vol. 9, No. 12, (February 2007), pp. 1438-1452, ISSN 1463-9084

Andreasen, A., Sørensen, M., Burkarl, R., Møller, B., Molenbroek, A., Pedersen, A., Vegge, T. & Jensen, T. (2006). Dehydrogenation kinetics of air-exposed MgH_2/Mg_2Cu and $MgH_2/MgCu_2$ studied with in situ X-ray powder diffraction. *Applied Physics A,* Vol. 82, No. 3, (February 2006), pp. 515-521, ISSN 1432-0630

Ansara, I., Dinsdale, A. & Rand, M. (Ed(s)). (1998). *COST 507, Thermochemical database for light metal alloys,* Vol. 2, pp. 170-174, Office for Official Publications of the European Communities, ISBN 92-828-3902-8, Luxembourg

Beattie, S., Setthanan, U. & McGrady, G. (2011). Thermal desorption of hydrogen from magnesium hydride (MgH2): An in situ microscopy study by environmental SEM and TEM. *International Journal of Hydrogen Energy,* Vol. 36, No. 10, (May 2011), pp. 6014-6021, ISSN 0360-3199

Bösenberg, U., Ravnsbæk, D., Hagemann, H., D'Anna, V., Minella, B., Pistidda, C., Beek, W., Jensen, T., Bormann, R. & Dornheim, M. (2010). Pressure and Temperature Influence on the Desorption Pathway of the $LiBH_4$−MgH_2 Composite System. *The Journal of Physical Chemistry C,* Vol. 114, No. 35, (August 2010), pp. 15212-15217, ISSN 1932-7455

Braga, M., Acatrinei, A., Hartl, M., Vogel, S., Proffen, T. & Daemen, L. (2010a). New Promising Hydride Based on the Cu-Li-Mg system. *Journal of Physics: Conference Series*, Vol. 251, (December 2010), pp. 012040 [4 pages], ISSN 1742-6596

Braga, M., Wolverton, M., Llobet, A. & Daemen, L. (2010b). Neutron Scattering to Characterize Cu/Mg(Li) Destabilized Hydrogen Storage Materials. *Materials Research Society Symposium Proceedings,* Vol. 1262, pp. 1262-W03-05 (April 2010), ISSN 0272-9172

Braga, M., Ferreira, J., Siewenie, J., Proffen, Th., Vogel, S. & Daemen, L. (2010c). Neutron powder diffraction and first-principles computational studies of $CuLi_xMg_{2-x}$ ($x \cong 0{,}08$), $CuMg_2$, and Cu_2Mg. *Journal of Solid State Chemistry,* Vol. 183, No. 1, (January 2010), pp. 10-19, ISSN 0022-4596

Braga, M. & Malheiros, L. (2007a). $CuMg_{2-Y}Li_X$ alloy for hydrogen storage. International patent, WO 2007046017 (A1)

Braga, M. & Malheiros, L. (2007b). $CuMg_{2-Y}Li_X$ alloy for hydrogen storage. National patent, PT 103368 (A)

Braga, M., Ferreira, J. & Malheiros, L. (2007). A ternary phase in Cu–Li–Mg system. *Journal of Alloys and Compounds,* Vol. 436, No. 1-2, (June 2007), pp. 278-284, ISSN 0925-8388

Cermak, J. & David, B. (2011). Catalytic effect of Ni, Mg_2Ni and Mg_2NiH_4 upon hydrogen desorption from MgH_2. *International Journal of Hydrogen Energy,* Vol. 36, No. 21, (October 2011), pp. 13614-13620, ISSN 0360-3199

Chen, P. & Zhu, M. (2008). Recent progress in hydrogen storage. *Materials Today,* Vol. 11, No. 12, (December 2008), pp. 36-43, ISSN 1369-7021

Chen, P., Xiong, Z., Luo, J., Lin, J. & Tan, K. (2003). Interaction between lithium amide and lithium hydride. *The Journal of Physical Chemistry B,* Vol. 107, No. 37, (September 2003), pp. 10967-10970, ISSN 1520-5207

Choi, Y., Hu, J., Sohn, H. & Fang, Z. (2008). Hydrogen storage properties of the Mg–Ti–H system prepared by high-energy–high-pressure reactive milling. *Journal of Power Sources,* Vol. 180, No. 1, (May 2008), pp. 491-497, ISSN 0378-7753

Churchard, A., Banach, E., Borgschulte, A., Caputo, R., Chen, J., Clary, D., Fijalkowski, K., Geerlings, H., Genova, R., Grochala, W., Jaroń, T., Juanes-Marcos, J., Kasemo, B., Kroes, G., Ljubić, I., Naujoks, N., Nørskov, J., Olsen, R., Pendolino, F., Remhof, A., Románszki, L., Tekin, A., Vegge, T., Zäch, M., & Züttelc, A. (2011). A multifaceted approach to hydrogen storage. *Physical Chemistry Chemical Physics,* Vol. 13, No. 38, (September 2011), pp. 16955-16972, ISSN 1463-9084

Cui, S., Feng, W., Hu, H., Feng, Z. & Wang, Y. (2008). Structural phase transitions in MgH_2 under high pressure. *Solid State Communications,* Vol. 148, No. 9-10, (December 2008), pp. 403-405, ISSN 0038-1098

David, W., Jones, M., Gregory, D., Jewell, C., Walton, A. & Edwards, P. (2007). A mechanism for non-stoichiometry in the lithium amide/lithium imide hydrogen storage reaction. *Journal of the American Chemical Society,* Vol. 129, No. 6, (February 2007), pp. 1594-1601, ISSN 0002-7863

Egami, T. & Billinge, S. (2003). *Underneath the Bragg-Peaks: Structural Analysis of Complex Materials* (First edition), Pergamon Press, Elsevier Ltd, ISBN 0-08-042698-0, Amsterdam

Elsasser, C., Krimmel, H., Fahnle, M., Louie, S. & Chan, C. (1998). *Ab initio* study of iron and iron hydride: III. Vibrational states of H isotopes in Fe, Cr and Ni. *Journal of Physics: Condensed Matter,* Vol. 10, No. 23, (June 1998), pp. 5131 [16 pages], ISSN 0953-8984

European Commission (2003). World energy, technology and climate policy outlook 2030 — WETO, in: *Directorate-General for Research Energy, EUR 20366*, Available from: http://ec.europa.eu/research/energy/pdf/weto_final_report.pdf

Farrow, C., Juhas, P., Liu, J., Bryndin, D., Božin, E., Bloch, J., Proffen, T. & Billinge, S. (2007). PDFfit2 and PDFgui: computer programs for studying nanostructure in crystals. *Journal of Physics: Condensed Matter,* Vol. 19, No. 33, (July 2007), pp. 335219 [7 pages], ISSN 0953-8984

Felderhoff, M., Weidenthaler, C., von Helmoltb, R. & Eberleb, U. (2009). Hydrogen storage: the remaining scientific and technological challenges. *Physical Chemistry Chemical Physics,* Vol. 9, No. 21, (May 2007), pp. 2643-2653, ISSN 1463-9084

Fernández, A., Deprez, E. & Friedrichs, O. (2011). A comparative study of the role of additive in the MgH_2 vs. the $LiBH_4$–MgH_2 hydrogen storage system. *International Journal of Hydrogen Energy,* Vol. 36, No. 6, (March 2011), pp. 3932-3940, ISSN 0360-3199

Fukai, Y. (1993). *The Metal-Hydrogen System: Basic Bulk Properties* (First edition), Springer-Verlag, ISBN 3540-556370, Berlin

Gibb, T. & Kruschwitz, H. (1950). The Titanium-Hydrogen System and Titanium Hydride. I. Low-Pressure Studies. *Journal of American Chemical Society*, Vol. 72, No. 12 pp. 5365-5369

Grochala, W. & Edwards, P. (2004). Thermal Decomposition of the Non-Interstitial Hydrides for the Storage and Production of Hydrogen. *Chemical Reviews,* Vol. 104, No. 3, (March 2004), pp. 1283-1315, ISSN 0009-2665

Hlukhyy, V., Rodewald, U. & Pöttgen, R. (2005). Magnesium-Tin Substitution in $NiMg_2$. *Zeitschrift für anorganische und allgemeine Chemie,* Vol. 631, No. 15, (November 2005), pp. 2997–3001, ISSN 1521-3749

Hohenberg, P. & Kohn, W. (1964). Inhomogeneous Electron Gas. *Physical Review B*, Vol. 136, No. 3B, (November 1964) pp. B864-B871, ISSN 1098-0121

Hong, S., Bae, J., Kwon, S. & Song, M. (2011). Hydrogen storage properties of Mg-23.5Ni-xCu prepared by rapid solidification process and crystallization heat treatment. *International Journal of Hydrogen Energy,* Vol. 36, No. 3, (February 2011), pp. 2170-2176, ISSN 0360-3199

Hsu, F., Hsu, C., Chang, J., Lin, C., Lee, S. & Jiang, C. (2010). Structure and hydrogen storage properties of $Mg_2Cu_{1-x}Ni_x$ (x = 0–1) alloys. *International Journal of Hydrogen Energy,* Vol. 35, No. 24, (December 2010), pp. 13247-13254, ISSN 0360-3199

Huot, J., Liang, G., Boily, S., Neste, A. & Schulz, R. (1999). Structural study and hydrogen sorption kinetics of ball-milled magnesium hydride. *Journal of Alloys and Compounds,* Vol. 293-295, (December 1999), pp. 495-500, ISSN 0925-8388

Jain, I., Lal, C. & Jain, A. (2010). Hydrogen storage in Mg: A most promising material. *International Journal of Hydrogen Energy,* Vol. 35, No. 10, (May 2010), pp. 5133-5144, ISSN 0360-3199

Jain, I. (2009). Hydrogen the fuel for 21st century. *International Journal of Hydrogen Energy,* Vol. 34, No. 17, (September 2009), pp. 7368-7378, ISSN 0360-3199

Jeon, K., Moon, H., Ruminski, A., Jiang, B., Kisielowski, C., Bardhan, R. & Urban, J. (2011). Air-stable magnesium nanocomposites provide rapid and high-capacity hydrogen storage without using heavy-metal catalysts. *Nature Materials,* Vol. 10, No. 4, (April 2011), pp. 286-290, ISSN 1476-4660

Jurczyk, M., Nowak, M., Szajek, A. & Jezierski, A. (2011). Hydrogen storage by Mg-based nanocomposites. *International Journal of Hydrogen Energy,* (In press - available online 27 April 2011), doi:10.1016/j.ijhydene.2011.04.012, ISSN 0360-3199

Jurczyk, M., Okonska, I., Iwasieczko, W., Jankowska, E. & Drulis H. (2007). Thermodynamic and electrochemical properties of nanocrystalline Mg_2Cu-type hydrogen storage materials. *Journal of Alloys and Compounds,* Vol. 429, No. 1-2, (February 2007), pp. 316-320, ISSN 0925-8388

Kalinichenka, S., Röntzsch, L., Riedl, T., Gemming, T., Weißgärber, T. & Kieback, B. (2011). Microstructure and hydrogen storage properties of melt-spun Mg–Cu–Ni–Y alloys. *International Journal of Hydrogen Energy,* Vol. 36, No. 2, (January 2011), pp. 1592-1600, ISSN 0360-3199

Larson, A., von Dreele, R. (2004). GSAS Generalized Structure Analysis System, LANSCE, Los Alamos.

Massa, W. (2008). *Crystal Structure determination.* Springer-Verlag, Berlin Heidelberg. ISBN 978-3540206446

Milanese, J., Girella, A., Garroni, S., Bruni, G., Berbenni, V., Matteazzi, P. & Marini, A. (2010a). Effect of C (graphite) doping on the H_2 sorption performance of the Mg–Ni storage system. *International Journal of Hydrogen Energy,* Vol. 35, No. 3, (February 2010), pp. 1285-1295, ISSN 0360-3199

Milanese, C., Girella, A., Bruni, G., Cofrancesco, P., Berbenni, V., Matteazzi, P. & Marini, A. (2010b). Mg-Ni-Cu mixtures for hydrogen storage: A kinetic study. *Intermetallics,* Vol. 18, No. 2, (February 2010), pp. 203-211, ISSN 0966-9795

Milanese, C., Girella, A., Bruni, G., Cofrancesco, P., Berbenni, V., Villa, M., Matteazzi, P. & Marini, A. (2008). Reactivity and hydrogen storage performances of magnesium–nickel–copper ternary mixtures prepared by reactive mechanical grinding. *International Journal of Hydrogen Energy,* Vol. 33, No. 17, (September 2008), pp. 4593-4606, ISSN 0360-3199

Noritake, T., Towata, S., Aoki, M., Seno, Y., Hirose, Y., Nishibori, E., Takata, M. & Sakata, M. (2003). Charge density measurement in MgH_2 by synchrotron X-ray diffraction. *Journal of Alloys and Compounds,* Vol. 356-357, (August 2003), pp. 84-86, ISSN 0925-8388

Orimo, S. & Fujii, H. (2001). Materials science of Mg-Ni-based new hydrides. *Applied Physics A,* Vol. 72, No. 2, (April 2001), pp. 167-186, ISSN 1432-0630

Ramirez-Cuesta, A. (2004). aCLIMAX 4.0. 1, The new version of the software for analyzing and interpreting INS spectra. *Computer Physics Communications.* Vol. 157, No. 3, pp. 226-238.

Ravindran, P., Vajeeston, P., Fjellvåg, H. & Kjekshus, A. (2004). Chemical-bonding and high-pressure studies on hydrogen-storage materials. *Computational Materials Science,* Vol. 30, No. 3-4, (August 2004), pp. 349-357, ISSN 0927-0256

Reilly, J. & Wiswall, R. (1967). The Reaction of Hydrogen with Alloys of Magnesium and Copper. *Inorganic chemistry,* Vol. 6, No. 12, (December 1967), pp. 2220-2223, ISSN 0020-1669

Reilly, J. & Wiswall, R. (1968). The Reaction of Hydrogen with Alloys of Magnesium and Nickel and the Formation of Mg_2NiH_4. *Inorganic chemistry,* Vol. 7, No. 11, (November 1968), pp. 2254-2256, ISSN 0020-1669

Reule, H., Hirscher, M., Weißhardt, A. & Kronmüller, H. (2000). Hydrogen desorption properties of mechanically alloyed MgH_2 composite materials. *Journal of Alloys and Compounds,* Vol. 305, No. 1-2, (June 2000), pp. 246-252, ISSN 0925-8388

Ross, D. (2008). Neutron scattering studies for analysing solid state hydrogen storage, in: *Solid State Hydrogen Storage Materials and Chemistry* Walker, G. Ed. CRC Woodhead Publishing: Cambridge, England, pp. 135-172. ISBN 9781845692704

Rude, L., Nielsen, T., Ravnsbæk, D., Bösenberg, U., Ley, M., Richter, B., Arnbjerg, L., Dornheim, M., Filinchuk, Y., Besenbacher, F. & Jensen, T. (2011). Tailoring properties of borohydrides for hydrogen storage: A review. *Physica Status Solidi A,* Vol. 208, No. 8, (July 2011), pp. 1754-1773, ISSN 1862-6300

Sabitu, S., Gallo, G. & Goudy, A. (2010). Effect of TiH_2 and Mg_2Ni additives on the hydrogen storage properties of magnesium hydride. *Journal of Alloys and Compounds,* Vol. 499, No. 1, (June 2010), pp. 35-38, ISSN 0925-8388

Schimmel, H., Huot, J., Chapon, L., Tichelaar, F. & Mulder, F. (2005). Hydrogen Cycling of Niobium and Vanadium Catalyzed Nanostructured Magnesium. *Journal of the*

American Chemical Society, Vol. 127, No. 41, (September 2005), pp. 1438-14354, ISSN 0002-7863

Schlapbach, L. & Züttel, A. (2001). Hydrogen-storage materials for mobile applications. *Nature,* Vol. 414, (November 2001), pp. 353-358, ISSN 0028-0836

Senegas, J., Mikou, A., Pezat, M. & Darriet, B. (1984). Localisation et diffusion de l'hydrogene dans le systeme Mg_2Ni-H_2: Etude par RMN de $Mg_2NiH_{0,3}$ et Mg_2NiH_4. *Journal of Solid State Chemistry,* Vol. 52, No. 1, (March 1984), pp. 1-11, ISSN 0022-4596

Setten, M., Wijs, G. & Brocks, G. (2007). Ab initio study of the effects of transition metal doping of Mg_2NiH_4. *Physical Review B,* Vol. 76, (August 2007), pp. 075125 [8 pages], ISSN 1098-0121

Siegel, D., Wolverton, C. & Ozoliņš, V. (2007). Thermodynamic guidelines for the prediction of hydrogen storage reactions and their application to destabilized hydride mixtures. *Physical Review B,* Vol. 76, No. 13, (October 2007), pp. 134102 [6 pages], ISSN 1098-0121

Simičić, M., Zdujić, M., Dimitrijević, R., Nikolić-Bujanović, L. & Popović N.(2006). Hydrogen absorption and electrochemical properties of Mg_2Ni-type alloys synthesized by mechanical alloying. *Journal of Power Sources,* Vol. 158, No. 1, (July 2006), pp. 730-734, ISSN 0378-7753

Sohn, H. & Emami, S. (2011). Kinetics of dehydrogenation of the Mg–Ti–H hydrogen storage system. *International Journal of Hydrogen Energy,* Vol. 36, No. 14, (July 2011), pp. 8344-8350, ISSN 0360-3199

Squires, G. (1978). *Introduction to the theory of Thermal Neutron Scattering.* Dover Publications Inc., Mineola, New York, ISBN 978-0486694474

Suryanarayana, C. (2008). Recent developments in mechanical alloying. *Reviews on Advanced Materials Science,* Vol. 18, No. 3, (August 2008), pp. 203-211, ISSN 1605-8127

Tan, Z., Chiu, C., Heilweil, E. & Bendersky, L. (2011a). Thermodynamics, kinetics and microstructural evolution during hydrogenation of iron-doped magnesium thin films. *International Journal of Hydrogen Energy,* Vol. 36, No. 16, (August 2011), pp. 9702-9713, ISSN 0360-3199

Tan, X., Danaie, M., Kalisvaart, W. & Mitlin, D. (2011b). The influence of Cu substitution on the hydrogen sorption properties of magnesium rich Mg-Ni films. *International Journal of Hydrogen Energy,* Vol. 36, No. 3, (February 2011), pp. 2154-2164, ISSN 0360-3199

Vajo, J. (2011). Influence of nano-confinement on the thermodynamics and dehydrogenation kinetics of metal hydrides. *Current Opinion in Solid State & Materials Science,* Vol. 15, No. 2, (April 2011), pp. 52-61, ISSN 1359-0286

Vajo, J. & Olson, G. (2007). Hydrogen storage in destabilized chemical systems. *Scripta Materialia,* Vol. 56, No. 10, (May 2007), pp. 829-834, ISSN 1359-6462

Vajo, J., Mertens, F., Ahn, C., Bowman Jr., R. & Fultz, B. (2004). Altering Hydrogen Storage Properties by Hydride Destabilization through Alloy Formation: LiH and MgH_2 Destabilized with Si. *The Journal of Physical Chemistry B,* Vol. 108, No. 37, (August 2004), pp. 13977-13983, ISSN 1520-5207

Vyas, D., Jain, P., Khan, J., Kulshrestha, V., Jain, A. & Jain, I. (2011). Effect of Cu catalyst on the hydrogenation and thermodynamic properties of Mg_2Ni. *International Journal of*

Hydrogen Energy, (In press - available online 20 July 2011), doi:10.1016/j.ijhydene.2011.05.143, ISSN 0360-3199

Xia, G., Leng, H., Xu, N., Li, Z., Wu, Z., Du, J. & Yu, X. (2011). Enhanced hydrogen storage properties of $LiBH_4$—MgH_2 composite by the catalytic effect of $MoCl_3$. *International Journal of Hydrogen Energy,* Vol. 36, No. 12, (June 2011), pp. 7128-725, ISSN 0360-3199

Yakel, H. (1958). Thermocrystallography of higher hydrides of Titanium and Zirconium. *Acta Crystallographica,* Vol. 11, pp. 45-51

Yang, J., Sudik, A. & Wolverton, C. (2007). Destabilizing $LiBH_4$ with a Metal (M) Mg, Al, Ti, V, Cr, or Sc) or Metal Hydride (MH_2) MgH_2, TiH_2, or CaH_2). *The Journal of Physical Chemistry C,* Vol. 111, No. 51, (November 2007), pp. 19134-19140, ISSN 1932-7455

Yim, C., You, B., Na, Y. & Bae, J. (2007). Hydriding properties of Mg–xNi alloys with different microstructures. *Catalysis Today,* Vol. 120, No. 3-4, (February 2007), pp. 276-280, ISSN 0920-586

Yvon, K. & Renaudin, G. (2005). Hydrides: Solid State Transition Metal Complexes, In: *Encyclopedia of Inorganic Chemistry,* R. Bruce King (Editor-in-Chief), pp. 1814–1846, John Wiley & Sons Ltd, ISBN 0-470-86078-2, Chichester

Yu, X., Grant, D. & Walker, G. (2006). A new dehydrogenation mechanism for reversible multicomponent borohydride systems—The role of Li–Mg alloys. *Chemical Communications,* No. 37, (October 2006), pp. 3906-3908, ISSN 1359-7345

Zaluska, A., Zaluski, L., & Strom-Olsen, J. (1999a). Nanocrystalline magnesium for hydrogen storage. *Journal of Alloys and Compounds,* Vol. 288, No. 1-2, (June 1999), pp. 217-225, ISSN 0925-8388

Zaluska, A., Zaluski, L., & Strom-Olsen, J. (1999b). Synergy of hydrogen sorption in ball-milled hydrides of Mg and Mg_2Ni. *Journal of Alloys and Compounds,* Vol. 289, No. 1-2, (July 1999), pp. 197-206, ISSN 0925-8388

Zaluski, L., Zaluska, A. & Strom-Olsen, J. (1997). Nanocrystalline metal hydrides. *Journal of Alloys and Compounds,* Vol. 253-254, (May 1997), pp. 70-79, ISSN 0925-8388

Zhang, J. & Hu, Y. (2011). Decomposition of Lithium Amide and Lithium Imide with and without Anion Promoter. *Industrial & Engineering Chemistry Research,* Vol. 50, No. 13, (May 2011), pp. 8058–8064, ISSN 0888-5885

Zhang, Y., Li, B., Ren, H., Guo, S., Zhao, D. & Wang, X. (2010a). Microstructure and hydrogen storage characteristics of melt-spun nanocrystalline $Mg_{20}Ni_{10-x}Cu_x$ (x=0-4) alloys. *Materials Chemistry and Physics,* Vol. 124, No. 1, (November 2010), pp. 795-802, ISSN 0254-0584

Zhang, Y., Li, B., Ren, H., Guo, S., Zhao, D. & Wang, X. (2010b). Hydrogenation and dehydrogenation behaviours of nanocrystalline $Mg_{20}Ni_{10-x}Cu_x$ (x = 0−4) alloys prepared by melt spinning. *International Journal of Hydrogen Energy,* Vol. 35, No. 5, (March 2010), pp. 2040-2047, ISSN 0360-3199

Zhang, J., Zhou, D., He, L., Peng, P. & Liu J. (2009). First-principles investigation of Mg_2Ni phase and high/low temperature Mg_2NiH_4 complex hydrides. *Journal of Physics and Chemistry of Solids,* Vol. 70, No. 1, (January 2009), pp. 32-39, ISSN 0022-3697

Zhao-Karger, Z., Hu, J., Roth, A., Wang, D., Kübel, C., Lohstroh, W. & Fichtner, M. (2010). Altered thermodynamic and kinetic properties of MgH_2 infiltrated in microporous scaffold. *Chemical Communications,* Vol. 46, No. 44, (November 2010), pp. 8353-8355, ISSN 1359-7345